ISSN 29450861 - Journal of the Association of Greek Chemists – JAGC – Volume 2- Issue 1

Conformational characteristics decisive for their biological action of organotin metallotherapeutics using a combination of NMR methods and *in silico* calculations

N. Zoupanou[a], Christina N. Banti [b], Sotiris K. Hadjikakou [b], M.E Stathopoulou[b], S. Kiriakidi[a], Carlos Silva Lopez [c], Uroš Javornik[d] , Sotiris K. Hadjikakou [a] ,T.Mavromoustakos[a]

[a]Department of Chemistry, National and Kapodistrian University of Greece Zografou, 15771, Athens, Greece

[b]Section of Inorganic and Analytical Chemistry, Department of Chemistry, University of Ioannina, 45110 Ioannina, Greece

[c]Department of Organic Chemistry, University of Vigo, Lagoas-Marcosende Campus, Vigo, Spain

[d]Slovenian NMR Centre, National Institute of Chemistry of Ljubljana, Hajdrihova 19, Slovenia

DOI: 10.62579/JAGC0013

Abstract

This study involves the structure elucidation and conformational analysis of three synthetic metallotherapeutics organotin (IV) derivatives of cholic acid (CAH) with the formulate $R_3Sn(CA)$ (R= Ph- (**1**), *n*-Bu- (**2**)) and $R_2Sn(CA)_2$ (R= Me- (**3**)**.** The structures of compounds (**1**-**3**) were assigned using a combination of homonuclear and heteronuclear 2D NMR experiments. Subsequently, ^{119}Sn NMR experiments and semi-empirical quantum mechanic computations (method PM6) were applied to determine the geometry surrounding the tin atom. Results showed that their optimized geometry is distorted tetrahedral and thus their biological activity of these compounds may be related with the conformation of atoms which endue the metal of Sn. *In silico* molecular docking studies were performed to the ER-α (estrogen receptor alpha ligand) justifying the compounds' biological activity.

Key Words : metallotherapeutics, organotin, NMR spectroscopy, semi-empirical quantum mechanic computations

INTRODUCTION

Metallotherapeutic compounds, in particular metal complexes, present an increasing interest in the field of medicinal chemistry. Their unique characteristics, such as redox activity, variable mode of coordination, antineoplastic properties and reactivity [1][2][3] to the organic substrate, make them attractive molecules in designing metallotherapeutics. Studies have shown that metallotherapeutic compounds could indicate significant action as anti-cancer agents, antibiotics and antibacterials[4]. Equally important is their role as medical and diagnostic factors too. Their obvious utility leads to the necessity for a further synthesis and thorough structure and conformational analysis, aiming to an optimized version of them with reduced serious side effects. According to similar studies Organotin (IV) complexes are associated with anti-proliferative activity, they have the ability to show better excretion from the body, cells do not develop resistance to them, and they also exhibit low toxicity levels. These factors make them valuable leads in the field of medicine [5][6][7][8][9].

According to many studies available in the literature, the biological activity and the role of the anti-cancer tin (IV) complexes, depend on the number and the type of group R, which bind to Sn [3]. Organotin (IV) compounds, which bound to carboxyl groups, provide antiproliferative properties too. Despite the cytotoxicity studies of organotin compounds (IV) against cancer cells, there is not much data on in vitro toxicity against healthy cells. In this context, it

has been found that certain compounds of di- and tri-organotin (IV) showed remarkably selective activity against cancer cell lines (HCT-116 and MCF-7) from normal cells. The results obtained from the studies and tests carried out in the field of organotin (IV) compounds seemed extremely interesting, starting a new era of research on the antiproliferative and anti-cancer activity of tin compounds. Small tri-organotin (IV) molecules have been shown to have better anti-cancer activity than their respective di-organotin (IV) derivatives, while among tri-organotin (IV) derivatives, triphenyl derivatives show improved activity [10][11][12].

In this study synthetic organotin (IV) compounds include the tin atom complexed with a different group R (R = Me, Bu, Phe) (**Figure 1**). In particular, the compounds that were analyzed were organotin (IV) derivatives of cholic acid (CAH) with the formulae $R_3Sn(CA)$ (R= Ph- (**1**), *n*-Bu- (**2**)) and $R_2Sn(CA)_2$ (R= Me- (**3**)). The combination of a strong antitumor agent, such as organotins, with the molecule of cholic acid, which exhibits hormone conformation, could contribute to a new formulation with selective activity against hormone depended tumour cells [13][14]. Compounds **1-3** were tested for their *in vitro* bioactivity against MCF-7 (positive to hormone receptors) and MDA-MB-231 (negative to hormone receptors) cells. The *in vitro* toxicity of **1-3** was evaluated towards MRC-5, while their *in vitro* genotoxicity was tested by the MN assay. The *in vivo* toxicity of **1-3** was tested by *Artemia salina* assay, while the *in vivo* genotoxicity by *Allium cepa* test. Moreover, the molecular mechanism of **1-3** against essential intracellular components was examined by their (i) DNA binding affinity, (ii) LOX inhibitory activity and (iii) catalytic activity on the peroxidation of linoleic [15][16].

1-3 were structurally elucidated using 1D and 2D homonuclear and heteronuclear NMR experiments. Subsequently, the conformational analysis and recognition of complexes was completed through experiments ^{119}Sn NMR and semi-empirical quantum mechanic computations. Molecular docking and quantum mechanics and molecular mechanic computations (QM/MM) are methods utilized to study both the binding of molecules to potential receptors that they may act, as well as to find their optimal geometry. MD calculations could confirm the stability of the complexes and justified their biological activities as binders at the ER-α.

2. Material and Methods

NMR Analysis

All of the Organotin (IV) derivatives were synthesized in the lab of Inorganic Chemistry at University of Ioannina and their synthesis was published elsewhere [1]. The structural elucidation of protons and carbons of the compounds **(1-3**) was achieved using 700 MHz Bruker Avance III HD magnet equipped with an ultra-sensitive triple-resonance TCI cryoprobe, installed at Pharmaceutical Department of University of Patras. 5 mg of each compound were dissolved in 550ml of DMSO-d6. The experiments, performed using Bruker library pulse sequences, included homonuclear ^{1}H ,^{13}C, ^{13}C APT NMR, 2D COSY, 2D ROESY and heteronuclear 2D HSQC and 2D HMBC experiments. All measurements are carried out at 25°C, and the data are acquired and processed with the MestreNova [17] and TopSpin 3.5 [18] software. Finally, ^{119}Sn NMR experiments were performed at NMR Lab of Slovene using spectrometer of 300MHz (Unity Inova NMR) and DMSO-d6 solvent.

Semi-empirical Quantum Mechanic Computations

Semi-empirical quantum mechanics computation was an effective tool for the analysis of the geometry of molecules. The Neglect of Diatomic Differential Overlap (NDDO)-based semi-empirical method PM6 [19] was used in order to calculate the geometries of the coordination complexes under study. The choice of this method was based upon its suitability for computing metal coordination complexes since it takes into account both the adoption of Viotyuk's core-core diatomic interaction term [20] and Thiel's d-orbital approximation [21][22][23]. The starting geometry for each complex was guessed based upon the results of the performed ^{1}H-NMR and Mössbauer experiments [24], which have already performed. Initial structures were designed in Molden and were used as input for geometry optimization in the PM6

level of theory with the Gaussian 09 software [25]. Frequency calculations were performed in the optimized geometries in order to assure that the resulting structures correspond to global minima and not any transition states.

In silico Molecular Docking studies

In silico studies, have been performed on the estrogen receptor alpha (ER-a). The structures of the organotin (IV) derivatives derived by PM6 calculations were used as input structures for the docking studies. The crystal structure of the macromolecule/receptor was downloaded from Protein Data Bank (PDB: 1A52).

AutoDock Tools (ADT) 4.5 was utilized for preparing the ligands and protein, as well as for analyzing the results. Molecular docking calculations were conducted by AutoDock4. Regarding the protein preparation, parameters were adjusted and polar hydrogen's were added to the receptor. Gasteiger charges were assigned to the protein's structure. Grid was generated based on coordinates the entire protein (blind docking) while, the grid box size was set to 126 Å in all directions. The center of the grid box was set to the active site, which was acquired by the cocrystallised ligand (estradiol), included in the crystal structure with the cod 1A52.

Docking software AutoDock4 and Autogrid4 algorithms were implemented in order to generate the grid maps.

Also, the parameters for Sn (IV) were extracted from the literature and were manually incorporated in AutoDock's parameter files. Finally, docking calculations were performed using the Genetic algorithm, determining the conformation of each complex with the most suitable binding mode to the receptor.

3.Strategy and results

The structure of molecules under study, contain one or two cholic acids and one different group R for each compound. The structures of complexes are shown below, and the strategy used for the structural identification of protons and carbons of the compounds (**1-3**) follows at **Figure 1**.

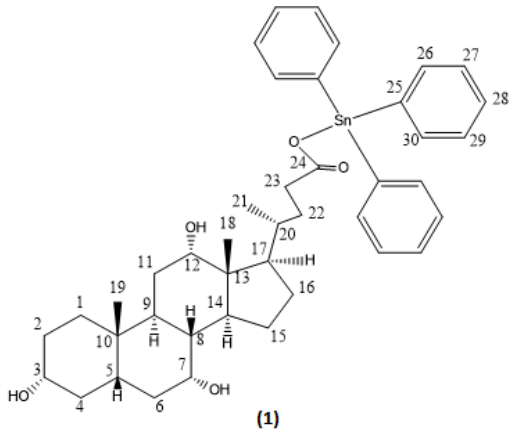

(1)

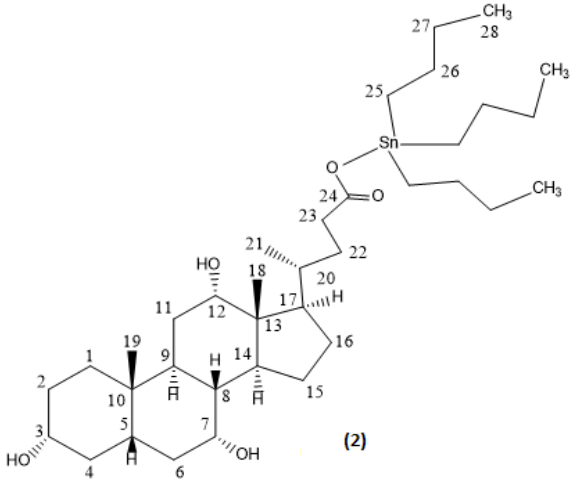

(2)

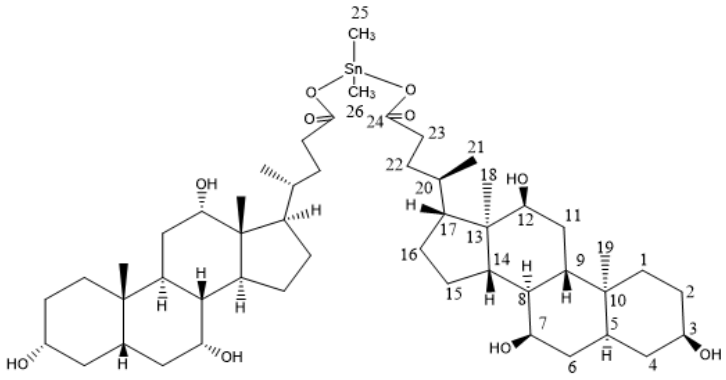

3.1 NMR analysis of compound 1

As a starting point for the structure elucidation, analyzing the NMR spectra of compound **1,** was taken the double peak of H21 (0.82ppm), which corresponds to CH_3. Through the combination of 2D HSQC and 2D COSY experiments, C21, H20 and C20, have been determined and they are resonated at 41.52ppm, 1.16ppm and 31.07ppm correspondingly. The second starting step is the singlet at 0.49 ppm, which corresponds to CH_3 H18. This was confirmed by the 2D HMBC spectrum which showed correlation of H18 with C12 resonated at 71.02ppm. Through 2D HSQC and 2D COSY confirmed the chemical shifts of H12 (3.74ppm) and OH12 (4.04ppm) were confirmed. The other singlet peak of CH_3 at 0.80ppm corresponds to H19. Through 2D HSQC it was found the C19 resonating at 22.64ppm.

Then next step in the strategy was the identification of H20. In particular, H20 at 2D COSY spectrum had correlation with protons which resonated at 1.70ppm and at 1.09ppm. According to the structure of molecule, these protons must be H17 and H22. Using the 2D HMBC spectrum, the already identified C18 correlated with proton at 1.70ppm, confirming its identity as H17. Therefore, H22 resonated at 1.09ppm. Through 2D HSQC C17 and C22 were identified. As H22 included two protons, the second H22 was identified using the 2D HSQC spectrum resonating at 1.60ppm. Apparently, through the 2D COSY experiment, the H23 protons were identified to resonate at 1.94ppm and 2.04ppm. C23 was identified through 2D HSQC.

A following step was to utilize identified C17 which through the 2D HMBC, correlated with proton H14 (1.93ppm). Using the 2D HSQC, C14 was determined. Through 2D COSY H14 correlated with H8 and this with H7 which subsequently correlated with OH7. Through 2D HSQC experiments C8 and C7 have been determined to resonate at 39.95ppm, 66.26ppm correspondingly. Identified H14 correlated through bond with H15 which resonated at 0.88ppm, and H15 with H16 which resonated at 1.67ppm. The second protons of H15 and H16 were revealed by 2D HSQC experiment.

Through the identified H7 and using 2D COSY experiment H6-H1 were identified and subsequently through 2D HSQC C6-C1. Then, through 2D HMBC experiment, identified C7 correlated with H9, which resonated at 2.09ppm. 2D COSY allowed through identified H9 to assign H11 (1.31ppm) and 2D HSQC the identification of C11.

It followed the identification of the triphenyl group. H28, is expected to show triplet, at the range of 7.38-7.42 ppm. The rest of the protons, H26/30 as a doublet and H27/29 as a doublet of doublets have been observed at 7,77ppm and 7,38-7,42ppm correspondingly. The carbons bearing protons have been identified through 2D HSQC and the tertiary C25 resonated at 143,38ppm according to 2D HMBC. The results of the analysis, the correlations of protons with carbons and the proton and carbon chemical shifts, are shown analytically in the following **Table 1**. At **Figure 2 and 3** are presented the ^{1}H NMR spectrum and the ^{13}C NMR spectrum analytically.

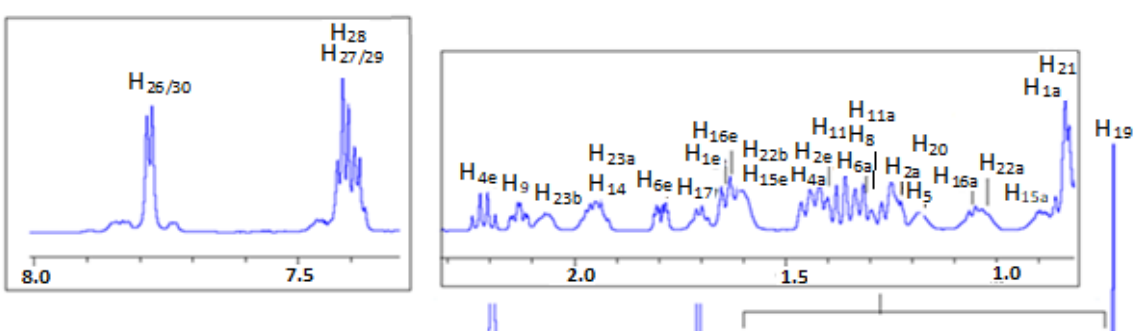

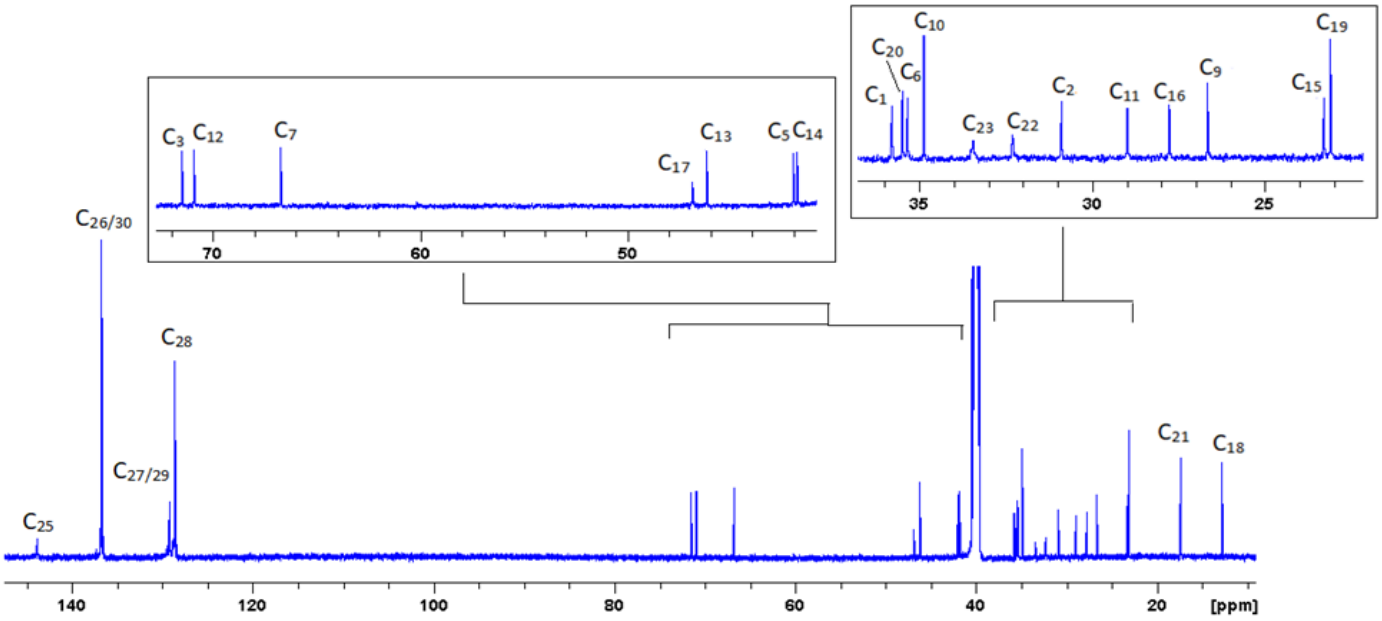

Figure 2: ^{13}C NMR spectrum of compound **1** obtained at ambient temperature in DMSO-d6 using 700 MHz Bruker NMR spectrometer.

Table 1. Chemicals Shifts of protons and carbons of compound (1) expressed in ppm.

Position	^{1}H (ppm)	^{13}C (ppm)	Position	^{1}H (ppm)	^{13}C (ppm)
1a	0.83	35.31	16a	1.04	27.35
1e	1.63	35.31	16e	1.62	27.35
2a	1.25	30.41	17	1.70	46.46
2e	1.41	30.41	18	0.49	12.36
3	3.17	70.45	19	0.80	22.70
4a	1.44	-	20	1.16	35.07
4e	2.19	-	21	0.82	16.95
5	1.22	41.53	22b	1.00	31.89
6a	1.36	34.86	22a	1.59	31.89
6e	1.78	34.86	23b	1.94	33.05
7	3.60	66.26	23a	2.07	33.05
8	1.30	-	24	-	-
9	2.11	26.19	25	-	143.38
10	-	34.39	26	7.77	136.70
11a	1.31	28.50	27	7.38-7.42	128.76
11e	1.40	28.50	28	7.38-7.42	128.17
12	3.74	71.02	29	7.38-7.4	128.76
13	-	-	30	7.77	136.70
14	1.93	41.40	OH-3	4.31	-
15a	0.88	22.88	OH-7	3.98	-
15e	1.58	22.88	OH-12	4.05	-

3.2 NMR analysis of compound 2

The strategy of compound **2** involved the assignment of the triplet resonated at 0.85 ppm as H28, while the rest protons and carbons have been assigned through 2D COSY and 2D HSQC. Especially, through 2D COSY was recognized that H27, H26 and H25 resonated at 1.54ppm, 1.27ppm and 1.02ppm. proton and carbon chemical shifts are shown analytically at **Table 2** and the ^{1}H NMR and ^{13}C NMR spectra at **Figure 4 and 5**.

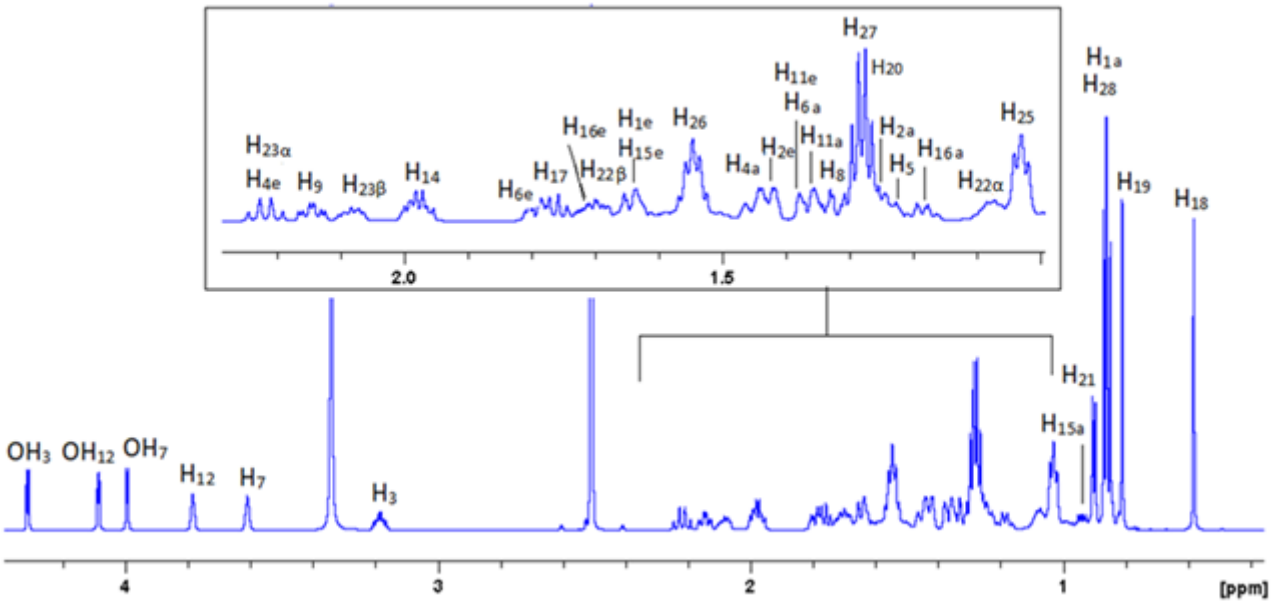

Figure 4: ^{1}H NMR spectrum of compound (**2)** obtained at ambient temperature in dmso-d6 and using 700 MHz Bruker NMR spectrometer.

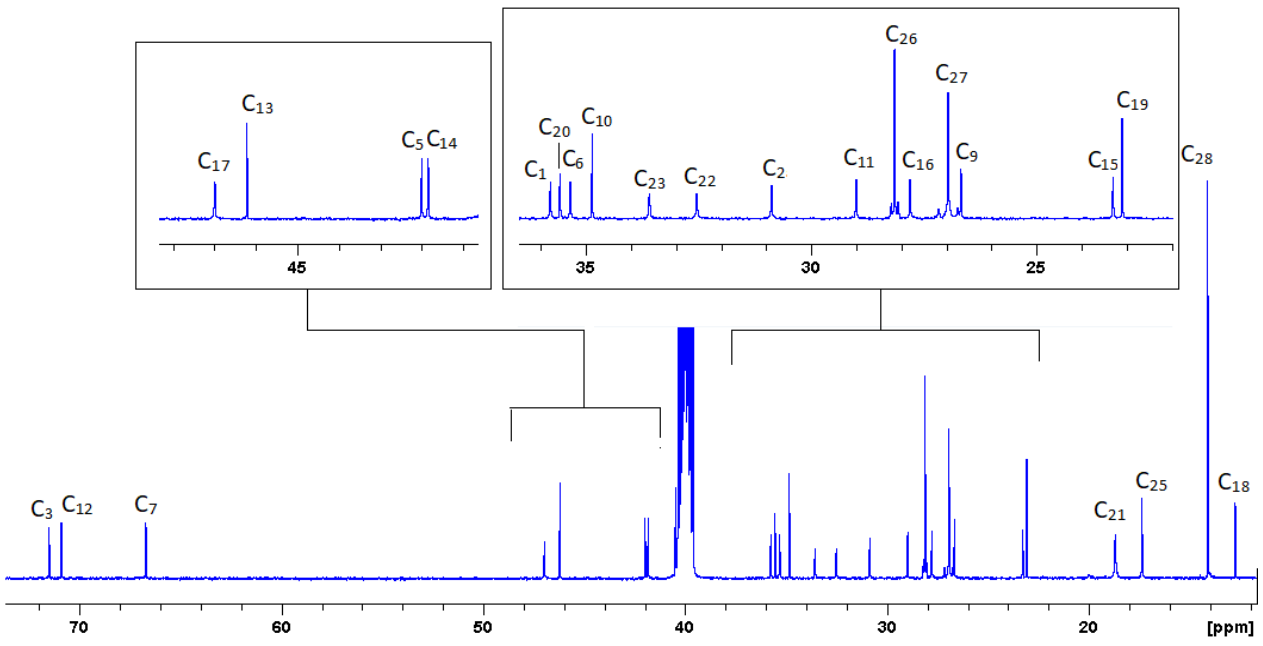

Figure 5: ^{13}C NMR spectrum of compound (**2)** obtained at ambient temperature in DMSO-d6 and using 700 MHz Bruker NMR spectrometer.

Table 2. Chemicals Shifts of protons and carbons of compound (2) expressed in ppm.

Position	^{1}H	^{13}C	Position	^{1}H	^{13}C
1e	1.63	35.38	15e	1.63	22.90
1a	0.83	35.38	16e	1.72	27.40
2e	1.42	30.46	16a	1.17	27.40
2a	1.25	30.46	17	1.76	46.59
3	3.18	70.53	18	0.58	12.37
4e	2.21	-	19	0.80	22.70
4a	1.44	-	20	1.28	35.16
5	1.22	41.60	21	0.90	17.00
6e	1.79	34.94	22a	1.67	32.14
6a	1.36	34.94	22b	1.07	32.14
7	3.60	66.33	23b	2.07	33.18
8	1.32	-	23a	2.20	33.18
9	2.14	26.28	24	-	177.76
10	-	34.45	25	1.02	18.31
11e	1.40	28.60	26	1.53	27.74
11b	1.34	28.60	27	1.27	26.56
12	3.79	71.12	28	0.85	13.73
13	-	45.81	OH-3	4.30	-
14	1.97	41.45	OH-7	3.99	H-7
15a	0.94	22.90	OH-12	4.09	H-12

3.3 NMR analysis of compound 3

Finally, chemical shifts of proton and carbon are shown at **Table 3** and the ^{1}H NMR and ^{13}C NMR spectra at **Figure 6 and Figure 7**. Finally, compound **3** involved an extra step, which involved the assignment of the singlet resonance at 0.66 ppm and which is assigned as H26, in particular at CH_3 (**Table 3**, **Figure 6 and 7).**

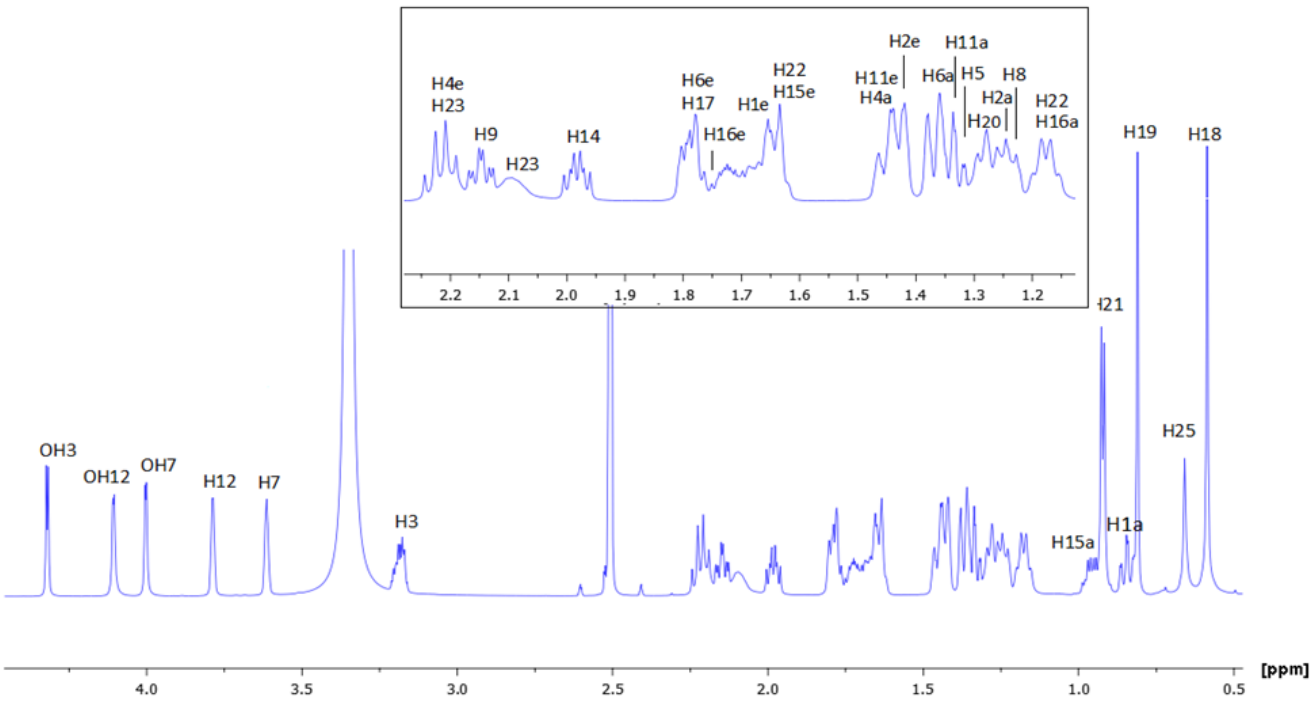

Figure 6: ^{1}H NMR spectrum of compound (3) obtained at ambient temperature in DMSO-d6 using 700 MHz Bruker NMR spectrometer.

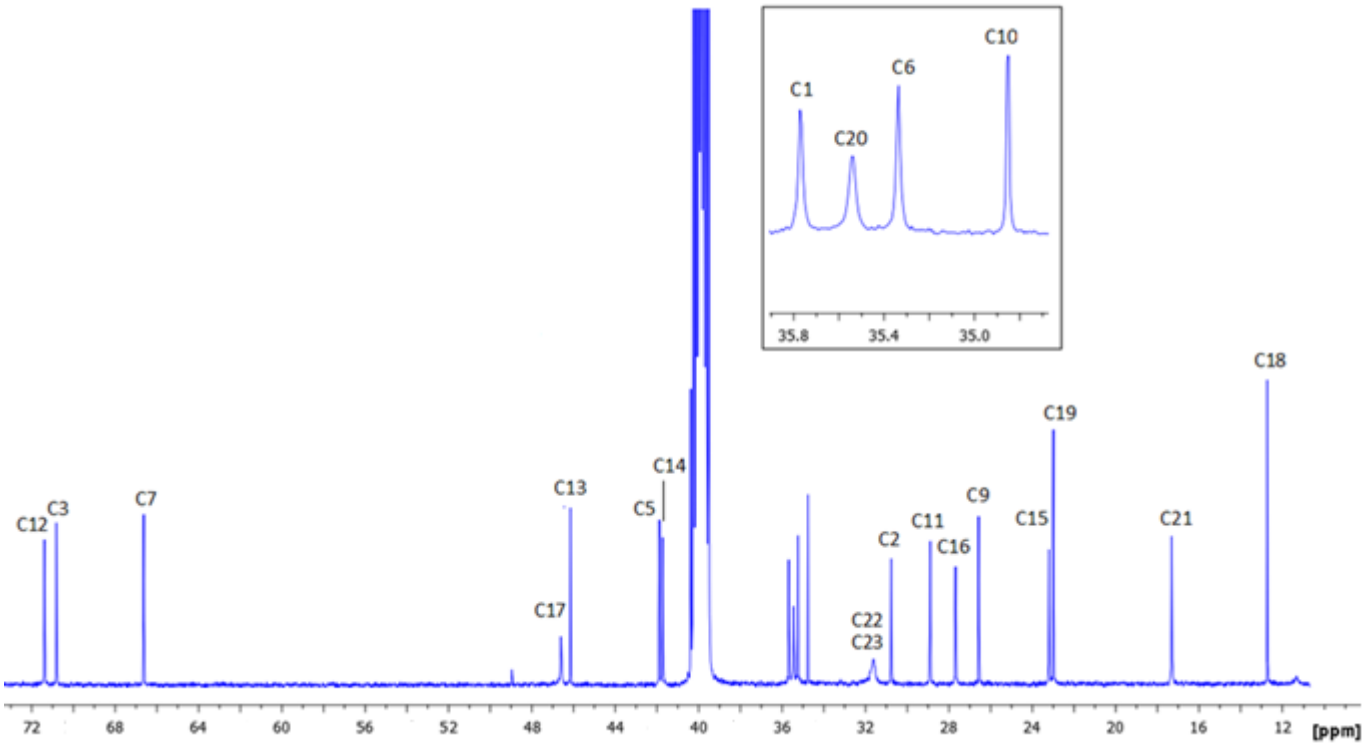

Figure 7: ^{13}C NMR spectrum of compound (3) obtained at ambient temperature in DMSO-d6 using 700 MHz Bruker NMR spectrometer.

Table 3. Chemicals Shifts of protons and carbons of compound (3) expressed in ppm.

Position	^{1}H	^{13}C	Position	^{1}H	^{13}C
1a	0.86	35.31	15e	1.63	2283
1e	1.63	35.31	16e	1.75	27.31
2e	1.42	30.57	16a	1.17	27.31
2a	1.25	30.57	17	1.77	46.24
3	3.18	70.44	18	0.59	12.35
4e	2.22	-	19	0.81	22.62
4a	1.44	-	20	1.28	35.08
5	1.22	41.52	21	0.92	16.94
6a	1.36	34.87	22b	1.17	34.39
6e	1.78	34.87	22a	1.64	34.39
7	3.61	66.26	23b	2.09	31.24
8	1.32	-	23a	2.20	31.24
9	2.14	26.20	24		
10	-	45.78	25	0.66	11.10
11a	1.34	28.95	26	0.66	-
11e	1.44	28.95	27		
12	379	71.01	OH-3	4.32	-
13	-	48.60	OH-7	4.00	-
14	1.98	41.36	OH-12	4.10	-
15a	0.94	22.83			

3.4 ^{119}Sn NMR analysis of compounds

^{119}Sn NMR experiments were performed to study its geometry with the surrounding substituents. The nature of the substituents determines the observed chemical shifts. Subsequently, the chemical shifts are correlated with certain geometries. The use of known spectroscopic data with determined geometries are in aid of this effort. ^{119}Sn NMR spectra were obtained in DMSO-d6 solvent. $SnCl_4$ was used as reference compound with known chemical shift (-150.41) (**Figure 8**).

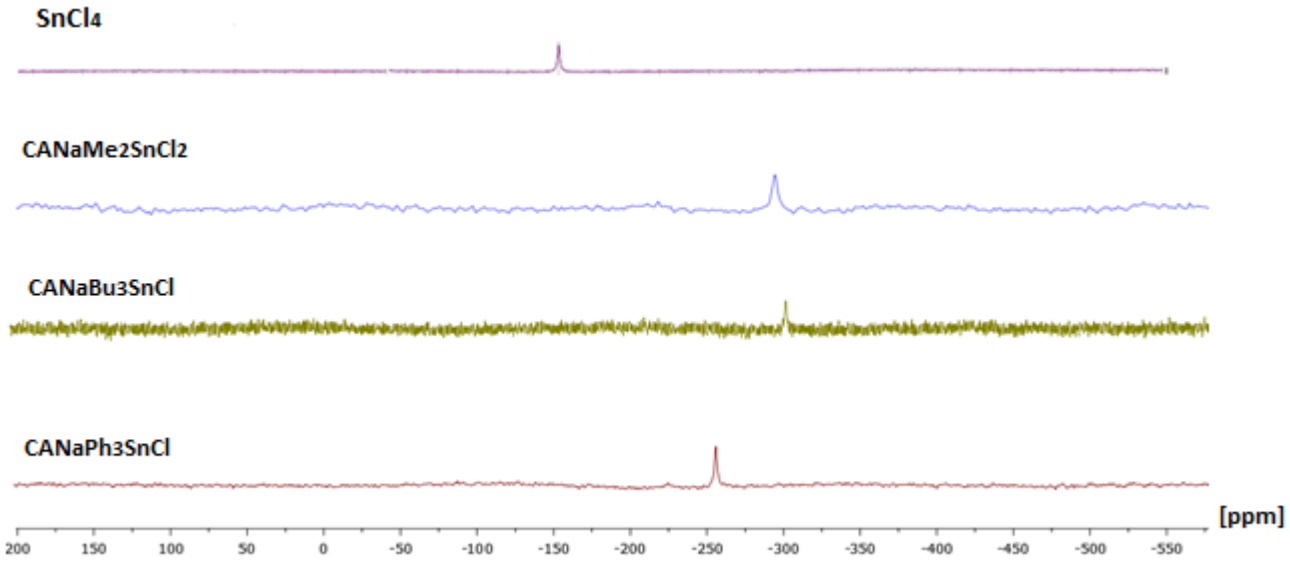

Figure 8. Spectra of ^{119}Sn NMR of compounds (**1**-**3**) and the reference compound $SnCl_4$.

According to the literature a four coordinated Sn provides a ^{119}Sn NMR spectrum shows resonances that range between -60 - 200 ppm [2-3] with a possible tetrahedral geometry [5]. The five-coordinated Sn gives peaks that resonate between -330ppm-(-) 90ppm, with a possible triangular dipyramid or tetrahedral dipyramid geometry [5]. Finally, a six-coordinated Sn gives peaks that resonated between -210ppm until -515ppm [2-3], with a possible octahedral geometry [5]. Based on these literature data the observed chemical shifts for the three complexes designate geometries shown in **Table 4**. [26][27][28][29]

Table 4. Chemical shifts observed with ^{19}Sn NMR spectroscopy for compounds (**1-3)** and their possible geometry according to literature data.

a/a	Compound	Chemical shift	Δδ to reference compound $SnCl_4$	Geometry of Compound
1	$SnCl_4$	-150.41	-	-
2	$CANaPh_3SnCl$	-257.44	107.04	triangular dipyramid or tetrahedral dipyramid or octahedral geometry
3	$CANaBu_3SnCl$	-305.82	155.50	triangular dipyramid or tetrahedral dipyramid or octahedral geometry
4	$CANaMe_2SnCl_2$	-294.61	144.21	triangular dipyramid or tetrahedral dipyramid or octahedral geometry

4. Semi-empirical quantum mechanic computations

Semi-empirical method PM6 was used in order to calculate the geometries of the coordination complexes under study. The starting geometry for each complex was guessed based upon the results of the performed ^{1}H-NMR and Mossbauer experiments. Initial structures were designed in Molden and were used as input for geometry optimizations in the PM6 level of theory with the Gaussian 09 software. Frequency calculations were performed in the optimized geometries in order to assure that the resulting structures correspond to global minima and not any transition states.
The resulting geometries of the coordination complexes under study are presented in **Table 5**.

Table 5. Bond lengths and relative angles for both organometallic complexes. The numbers 1,2 & 3 correspond either to butyl or phenyl groups depending on the structure. The complexes exhibit a distorted tetrahedral geometry with angles very close to the 109° of the perfect tetrahedron.

Structure	Bond(Å)				
	Sn-CANa (1)	Sn-CANa (2)	Sn-C1	Sn-C2	Sn-C3
$CANa(Bu)_3Sn$	2.13	-	2.15	2.15	2.15
$CANa(Ph)_3Sn$	2.12	-	2.12	2.12	2.12
$CANa(Me)_2Sn$	2.06	2.10	2.11	2.11	-

Table 6. Bond lengths and relative angles for both organometallic complexes. The numbers 1,2 & 3 correspond either to butyl or phenyl groups depending on the structure. The complexes exhibit a distorted tetrahedral geometry with angles very close to the 109° of the perfect tetrahedron.

Structure	(degrees)								
	C1-Sn-C2	C2-Sn-C3	C3-Sn-C1	C1-Sn-CANa (1)	C2-Sn-CANa (1)	C3-Sn-CANa (1)	C1-Sn-CANa (2)	C2-Sn-CANa (2)	CANa(1)-Sn-CANa(2)
$CANa(Bu)_3Sn$	113.79	114.83	116.02	105.78	98.39	105.52	-	-	-
$CANa(Ph)_3Sn$	114.39	116.10	114.07	106.02	107.03	96.63	-	-	-
$CANa(Me)_2Sn$	120.82	-	-	108.61	105.97	-	102.27	110.89	107.72

As it can be observed in **Figure 12**, all complexes exhibit a distorted tetrahedral geometry with angles very close to the 109° of the perfect tetrahedron.

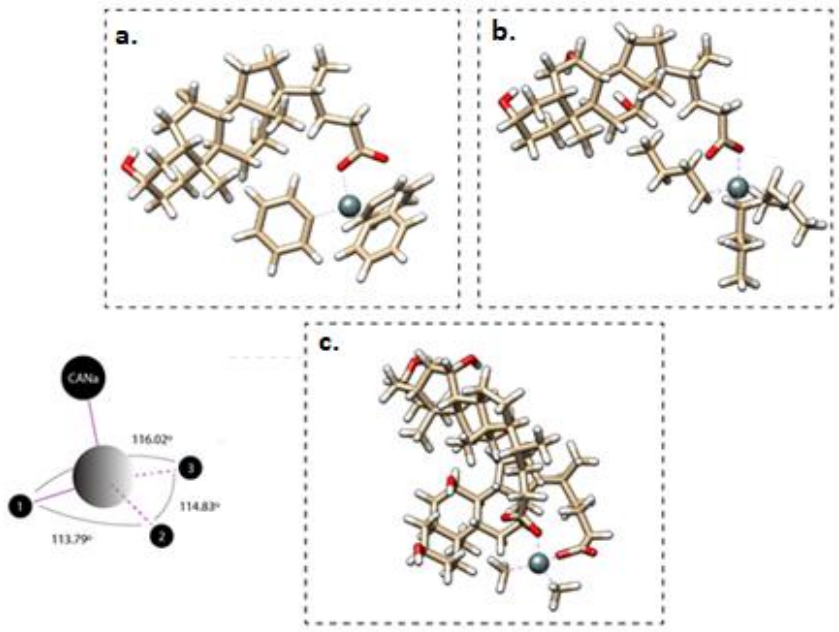

Figure 9. Schematic Representation of the PM6 geometry of $CANa(Ph)_3Sn$**(a),** $CANa(Bu)_3Sn$**(b)** and $CANa(Met)_2Sn$**(c)**. The geometry is distorted tetrahedral and the organometallic bonds are illustrated as purple dashed lines. A simplified version with some angle degrees are presented in the bottom left.

Interestingly, there is no agreement with the experimental data. A possible reason is that the solvent was not taken into account in the theoretical calculations.

5. Results of Molecular Docking Studies

The *in silico* experiments of molecular docking showed the binding of compounds **(1-3**) with the estrogen receptor (1a52). The molecular docking calculations were conducted three -times, in order to obtain reliable results. The average of the values of binding energy and binding constant (K_D), are presented at **Table 7**.

Table 7: Binding Energy, binding constant (K_D) values and H-bonds of molecular docking calculations.

Receptor 1a52 - Compounds	**Binding Energy Kcal/mol**	**Constant K_D**	H Bonds
Receptor 1a52/ complex 1	-9.94 ±0.5	0.003 nM	OH(3) with His 501 H(24) with Leu 509
Receptor 1a52/ complex 2	-6.52±0.5	0.010 μM	OH(3) with Glu 441 OH(3) with Asn 449 OH(7) with Glu 397
Receptor 1a52/ complex 3	-7.37±0.5	0.061 nM	OH(3) with Glu 330 OH(3) with Arg 352 OH(12) HOH 560

In all the "enzyme-ligand" complexes that were formed, the receptor (PDB:1A52) was interacting with the ligands through electrostatics and H-bond formation. The binding energy of all the complexes demonstrates a significantly strong energy. In particular, It was observed that the cholic acid binds in the active side of the receptor, creating H-bonds, between the OH(3) and H(24) of cholic acid to the amino acids His 501 and Leu 509 correspondingly **(Figure 10a).** The corresponding interactions for complex 2 with the receptor were H-bonds of OH(3) to amino acids Glu 441 and Asn 449 and OH(7) to amino acid Glu 397 as it is presented at **Figure 10b**. Complex 3 had interactions through H-bonds. In particular, the one cholic acid presented H-bond between OH(3)/OH(12) with Asp 351 and OH(7) with Lys 529. The other cholic acid had H-bonds between OH(3') and the amino acids Glu 330 and Arg 352 **(Figure 10c)**. The visualization of docking results were performed by Pymol program for all complexes.

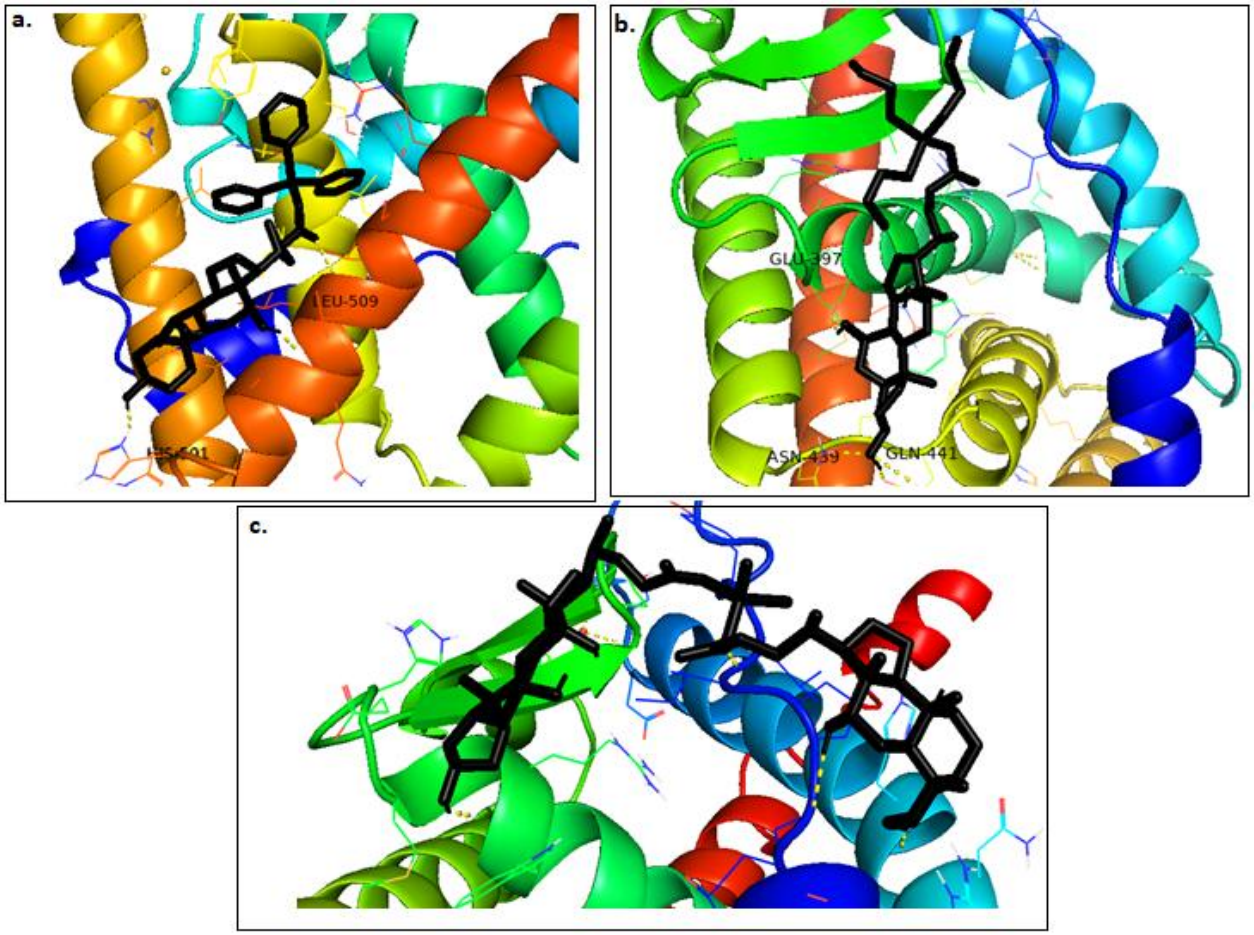

Figure 10. Interaction of complex **(1-3)** with the receptor (PDB:1a52).

6. Conclusions

In this study, we carried out the structural elucidation and conformational analysis of three synthetic organotin(IV) derivatives of cholic acid (CAH) with the general formulas $R_3Sn(CA)$ (R = Ph (1), n-Bu (2)) and $R_2Sn(CA)_2$ (R = Me (3)). To achieve this, we employed a combination of 1D and 2D homonuclear and heteronuclear NMR experiments along with ^{119}Sn NMR spectroscopy. Additionally, semi-empirical quantum mechanical calculations (PM6 method) were applied to investigate the geometry surrounding the tin atom. Their consistent results pointed out that their optimized geometry is distorted tetrahedral. This conformation may be responsible for their biological. To justify this, *in silico* molecular docking studies were performed to the ER-α (estrogen receptor alpha ligand). Their high binding affinity illustrates the possible relation between the putative bioactive conformation and possible bioactivity.

References

(1) N. Kaluderovic, G.; Paschke, R. Anticancer Metallotherapeutics in Preclinical Development. *Curr Med Chem* **2011**, *18* (31), 4738–4752. https://doi.org/10.2174/092986711797535308.

(2) Tabassum, S.; Yadav, S.; Arjmand, F. Exploration of Glycosylated-Organotin(IV) Complexes as Anticancer Drug Candidates. *Inorganica Chim Acta* **2014**, *423*, 38–45. https://doi.org/10.1016/j.ica.2014.07.080.

(3) Amir, M. K.; Khan, S.; Zia-ur-Rehman; Shah, A.; Butler, I. S. Anticancer Activity of Organotin(IV) Carboxylates. *Inorganica Chim Acta* **2014**, *423*, 14–25. https://doi.org/10.1016/j.ica.2014.07.053.

(4) Gielen, M. Tin-Based Antitumour Drugs. *Coord Chem Rev* **1996**, *151*, 41–51. https://doi.org/10.1016/S0010-8545(96)90193-9.

(5) Gielen, M. An Overview of Forty Years Organotin Chemistry Developed at the Free Universities of Brussels ULB and VUB. *J Braz Chem Soc* **2003**, *14* (6). https://doi.org/10.1590/S0103-50532003000600003.

(6) Pettinari, C.; Marchetti, F.; Pettinari, R.; Cingolani, A.; Drozdov, A.; Troyanov, S. The Interaction of Organotin(Iv) Acceptors with 1,4-Bis(5-Hydroxy-1-Phenyl-3-Methyl-1H-Pyrazol-4-Yl)Butane-1,4-DioneCoordination Chemistry of Bis(Pyrazolones): A Rational Design of Nuclearity Tailored Polynuclear Complexes. Part 2.22. *Journal of the Chemical Society, Dalton Transactions* **2002**, No. 2, 188–194. https://doi.org/10.1039/b106665j.

(7) Alama, A.; Tasso, B.; Novelli, F.; Sparatore, F. Organometallic Compounds in Oncology: Implications of Novel Organotins as Antitumor Agents. *Drug Discov Today* **2009**, *14* (9–10), 500–508. https://doi.org/10.1016/j.drudis.2009.02.002.

(8) Gielen, M. TIN-BASED ANTITUMOUR DRUGS. *Main Group Metal Chemistry* **1994**, *17* (1–4), 1–8. https://doi.org/10.1515/MGMC.1994.17.1-4.1.

(9) Gielen, M.; El Khloufi, A.; Biesemans, M.; Bouhdid, A.; de Vos, D.; Mahieu, B.; Willem, R. Synthesis, Characterization and High *In Vitro* Antitumour Activityof Novel Triphenyltin Carboxylates. *Met Based Drugs* **1994**, *1* (4), 305–309. https://doi.org/10.1155/MBD.1994.305.

(10) Pattan, S. R.; Pawar, S. B.; Vetal, S. S.; Gharate, U. D.; Bhawar, S. B. THE SCOPE OF METAL COMPLEXES IN DRUG DESIGN - A REVIEW. *INDIAN DRUGS* **2012**, *49* (11), 5–12. https://doi.org/10.53879/id.49.11.p0005.

(11) Stathopoulou, M. E. K.; Zoupanou, N.; Banti, C. N.; Douvalis, A. P.; Papachristodoulou, C.; Marousis, K. D.; Spyroulias, G. A.; Mavromoustakos, T.; Hadjikakou, S. K. Organotin Derivatives of Cholic Acid Induce Apoptosis into Breast Cancer Cells and Interfere with Mitochondrion; Synthesis, Characterization and Biological Evaluation. *Steroids* **2021**, *167*, 108798. https://doi.org/10.1016/j.steroids.2021.108798.

(12) Banti, C. N.; Hadjikakou, S. K.; Sismanoglu, T.; Hadjiliadis, N. Anti-Proliferative and Antitumor Activity of Organotin(IV) Compounds. An Overview of the Last Decade and Future Perspectives. *J Inorg Biochem* **2019**, *194*, 114–152. https://doi.org/10.1016/j.jinorgbio.2019.02.003.

(13) Willem, R.; Bouhdid, A.; Mahieu, B.; Ghys, L.; Biesemans, M.; Tiekink, E. R. T.; de Vos, D.; Gielen, M. Synthesis, Characterization and in Vitro Antitumour Activity of Triphenyl- and Tri-n-Butyltin Benzoates, Phenylacetates and Cinnamates. *J Organomet Chem* **1997**, *531* (1–2), 151–158. https://doi.org/10.1016/S0022-328X(96)06686-7.

(14) Schmiedgen, R.; Huber, F.; Preut, H.; Ruisi, G.; Barbieri, R. Synthesis and Characterization of Diorganotin(IV) Derivatives of 2-mercaptopyridine and Crystal Structure of Diphenyl Pyridine-2-thiolatochlorotin(IV). *Appl Organomet Chem* **1994**, *8* (4), 397–407. https://doi.org/10.1002/aoc.590080414.

(15) William Reusch. *Stereoisomers Part I, In Virtual Textbook of Organic Chemistry*; Michigan State University, 2010.

(16) Jaiswal, N.; Kushwaha, A. K.; Singh, A. P.; Dubey, R. K. Synthesis, Spectroscopic Characterization and Computational Studies of Schiff Base Complexes of Tin(IV) Chloride. *Main Group Metal Chemistry* **2019**, *42* (1), 28–36. https://doi.org/10.1515/mgmc-2019-0002.

(17) MestReNova. Mestrelab Research . S.L. Feliciano Barrera 9B, Bajo, 15706 Santiago de Compostela, Spain.

(18) TopSpin Software. 4.0-Bruker.

(19) Stewart, J. J. P. Optimization of Parameters for Semiempirical Methods V: Modification of NDDO Approximations and Application to 70 Elements. *J Mol Model* **2007**, *13* (12), 1173–1213. https://doi.org/10.1007/s00894-007-0233-4.

(20) Voityuk, A. A.; Rösch, N. AM1/d Parameters for Molybdenum. *J Phys Chem A* **2000**, *104* (17), 4089–4094. https://doi.org/10.1021/jp994394w.

(21) Thiel, W.; Voityuk, A. A. *Theoretica Chimica Acta Extension of the MNDO Formalism to d Orbitals: Integral Approximations and Preliminary Numerical Results*; 1992; Vol. 81.

(22) Thiel, W.; Voityuk, A. A. Extension of MNDO to d Orbitals: Parameters and Results for the Second-Row Elements and for the Zinc Group. *J Phys Chem* **1996**, *100* (2), 616–626. https://doi.org/10.1021/jp952148o.

(23) Thiel, W.; Voityuk, A. A. Extension of the MNDO Formalism Tod Orbitals: Integral Approximations and Preliminary Numerical Results. *Theor Chim Acta* **1992**, *81* (6), 391–404. https://doi.org/10.1007/BF01134863.

(24) Schaftenaar, G.; Vlieg, E.; Vriend, G. Molden 2.0: Quantum Chemistry Meets Proteins. *J Comput Aided Mol Des* **2017**, *31* (9), 789–800. https://doi.org/10.1007/s10822-017-0042-5.

(25) 34. M. J. Frisch, G. W. T. H. B. S. G. E. S. M. A. R. J. R. C. G. S. V. B. G. A. P. H. N. X. L. M. C. A. V. M. J. B. B. G. J. R. G. B. M. H. P. H. J. V. D. J. F. Gaussian 16, Revision B.01. *In Gaussian 09* **2016**.

(26) Holeček, J.; Nádvorník, M.; Handlíř, K.; Lyčka, A. 13C and 119Sn NMR Spectra of Di-n-Butyltin(IV) Compounds. *J Organomet Chem* **1986**, *315* (3), 299–308. https://doi.org/10.1016/0022-328X(86)80450-8.

(27) Otera, J. 119Sn Chemical Shifts in Five- and Six-Coordinate Organotin Chelates. *J Organomet Chem* **1981**, *221* (1), 57–61. https://doi.org/10.1016/S0022-328X(00)81028-1.

(28) Holeček, J.; Nádvorník, M.; Handlíř, K.; Lyčka, A. 13C and 119Sn NMR Study of Some Four- and Five-Coordinate Triphenyltin(IV) Compounds. *J Organomet Chem* **1983**, *241* (2), 177–184. https://doi.org/10.1016/S0022-328X(00)98505-X.

(29) Nádvorník, M.; Holeček, J.; Handlíř, K.; Lyčka, A. The 13C and 119Sn NMR Spectra of Some Four- and Five-Coordinate Tri-n-Butyltin(IV) Compounds. *J Organomet Chem* **1984**, *275* (1), 43–51. https://doi.org/10.1016/0022-328X(84)80576-8.

Acknowledgment: Sn^{2+} experiments have been performed in NMR center of NCI located in Ljubljana of Slovenia through CERI Program (20222161).